Mechanical heterogeneity in nanoscale films of liquid silica

Daniel J. Lacks and Michael-Paul Robinson
Department of Chemical Engineering, Case Western Reserve University, Cleveland, Ohio 44106, USA
(Received 28 October 2007; published 7 April 2008)

Molecular dynamics simulations are carried out for slabs of silica liquid with thicknesses between 1 and 3 nm. A local analysis of the Born contribution to the elastic modulus, C^B, shows that the elasticity is not uniform throughout the slabs—C^B is identical to that of bulk silica in the slab interior, but C^B is larger at the slab edges. The larger C^B at the slab edges is due to a distinct atomic level structure characterized by larger density, larger concentration of more highly coordinated ions, and smaller silica rings.

DOI: 10.1103/PhysRevE.77.041504 PACS number(s): 61.46.−w, 61.20.Ja, 62.20.D−

I. INTRODUCTION

Recent experiments on nanoporous amorphous silica suggest that nanostructuring may provide a way to create porous materials with more favorable mechanical properties. These nanoporous silica materials, produced from surfactant-templated self-assembly, have pores of 2 to 3 nm diameter that extend through an amorphous silica framework with walls of 1 to 2 nm thickness [1,2]. Nanoporous silica deforms more reversibly [3,4] and requires higher strains for failure [5] than bulk silica, and has elastic moduli that are less sensitive to porosity than natural porous solids [6].

To elucidate this unusual mechanical behavior, we examine how nanostructuring affects the *local* elasticity in liquid silica. Nanoscale structure is known to induce changes in the atomic-level structure of liquid silica, such that the structure near the surface differs from the bulk structure [7–9]. Since elasticity is determined by the atomic level structure, the local elasticity may be similarly heterogeneous.

Silica liquid, rather than silica glass, is studied here for two reasons: First, the properties of a liquid are well-defined because the liquid is in equilibrium, while the properties of a glass depend on its history (e.g., cooling rate). Second, it is much easier to obtain *well-averaged* results for the position dependence of local properties for a liquid than for a glass. The results for silica liquid will give insight into the behavior of silica glass because the structure of a glass is closely related to that of a liquid: As a liquid is cooled, the system dynamics slows and the atomic structure changes, and at the glass transition temperature the system becomes effectively trapped in the structure of the liquid at that point [10].

II. COMPUTATIONAL METHODS

Molecular dynamics simulations are carried out to obtain equilibrated liquid systems. The simulations are carried out at constant volume, with orthogonal simulation cells and periodic boundary conditions in all three dimensions. All simulations include 720 silicon atoms and 1440 oxygen atoms. The temperature is controlled with a Nose-Hoover thermostat, and the equations of motion are integrated by the fourth-order Runge-Kutta method with a time step of 2 fs. The simulations are carried out for durations of 1 ns.

The simulations are run at conditions corresponding to zero pressure. For the bulk system, a preliminary constant pressure simulation is run to determine the zero-pressure volume; a constant volume simulation is then carried out at this volume. Slabs of finite thickness in one dimension are simulated by setting one dimension of the simulation cell to be very large (50 Å), and the equilibrium slab thickness is varied by adjusting the other two dimensions of the simulation cell (with the number of atoms fixed); due to the vacuum that borders the slab, these simulation conditions correspond to zero pressure.

The atomic interactions are based on the van Beest-Kramer-van Santen (BKS) potential for silica [11]. The original BKS potential is modified in two ways. First, a steep repulsive wall that is significant only at very short interatomic distances is added [12], which is necessary because the short range repulsion in the BKS potential has a finite height that can be overcome in simulations at high temperatures. Second, the non-Coulombic potential is truncated at 5.5 Å and shifted in energy such that the energy is continuous at this cutoff distance [13], which leads to densities in better agreement with experiment. The Coulombic interactions are summed by the Ewald method.

The mechanical behavior is characterized here by the Born contribution to the elasticity, C^B, which is the second derivative of the potential energy with respect to uniform (affine) atomic displacements. While the total elastic modulus is the sum of the Born contribution, a stress fluctuation contribution, and a kinetic energy contribution, we do not address the stress fluctuation contribution because it is very slow to converge (especially for a local modulus), and we address the kinetic energy contribution only briefly because its effects are not as interesting. The value of C^B overestimates the true elastic modulus because the uniform atomic displacements are not the lowest energy atomic displacements; the stress fluctuation contribution accounts for deviations from uniform displacement (and thus is negative). The diagonal components of the Born contribution to the elastic modulus, C^B_{iiii}, are obtained from the simulations as

$$C^B_{iiii} = \frac{1}{V}\left\{\sum_{\alpha=1}^{N}\sum_{\beta=\alpha+1}^{N}\left(\frac{\partial^2 U}{\partial r_{\alpha\beta}^2} - \frac{1}{r_{\alpha\beta}}\frac{\partial U}{\partial r_{\alpha\beta}}\right)\left(\frac{(x_{\beta,i}-x_{\alpha,i})^4}{r_{\alpha\beta}^2}\right)\right\}, \tag{1}$$

where $x_{\alpha,i}$ is the coordinate of atom α along the i axis, $r_{\alpha\beta}$ is the distance between atoms α and β, U is the potential energy, V is the volume, and N is the number of atoms. The

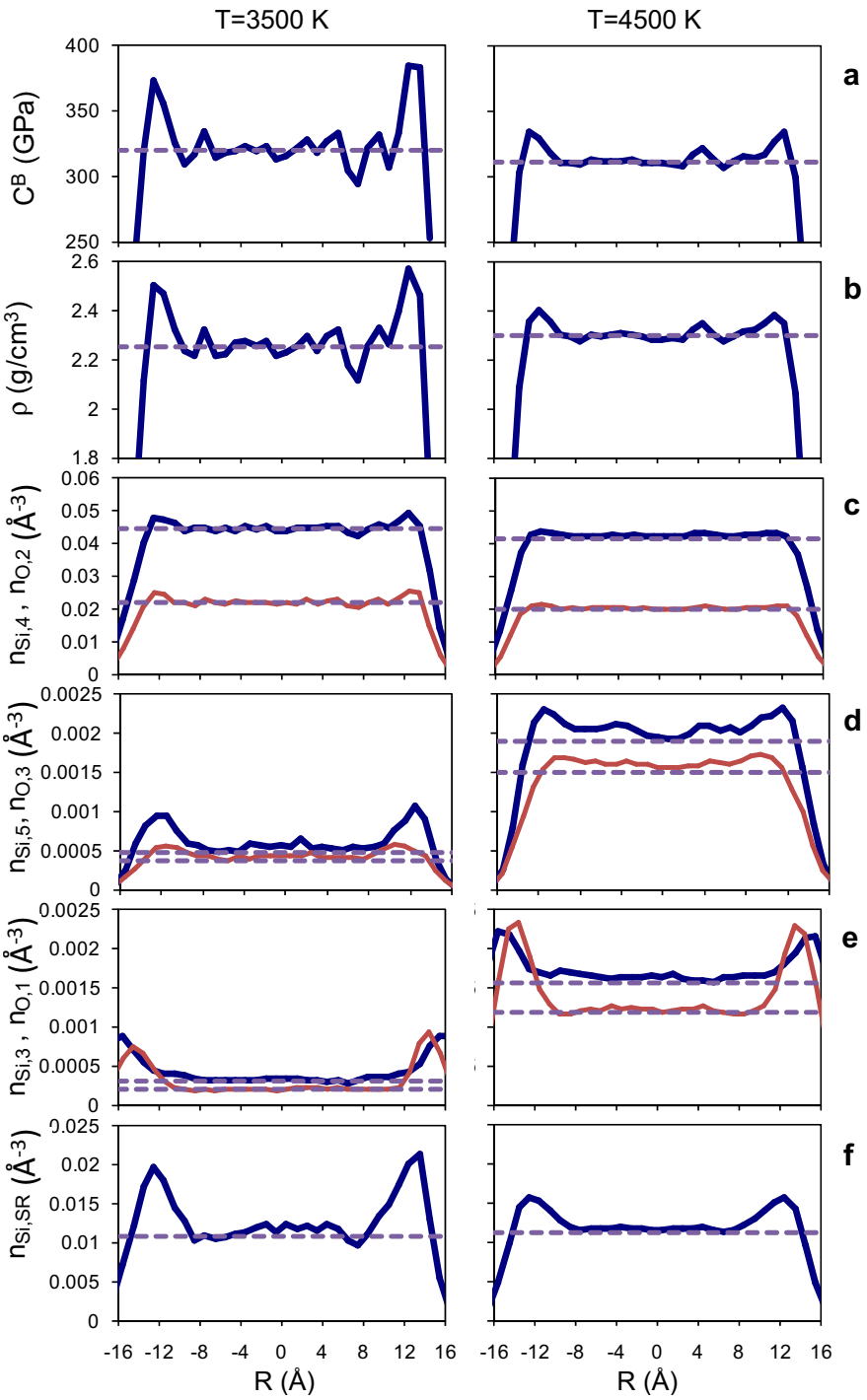

FIG. 1. (Color online) Results for properties as a function of position within the slab, for the slab with thickness of ~29 Å. Dashed lines represent results for bulk silica. Results at 3500 K are shown in the left panels, and results at 4500 K are shown in the right panels. (a) Born contribution to elastic modulus; (b) density; (c) number density of ions with normal coordination: Si with fourfold coordination (lower, brown curve) and O with twofold coordination (upper, blue curve); (d) number density of ions with higher coordination: Si with fivefold coordination (lower, brown curve) and O with threefold coordination (upper, blue curve); (e) number density of ions with lower coordination: Si with threefold coordination (lower, brown curve) and O with onefold coordination (upper, blue curve); and (f) number density of Si atoms that are part of a small ring (a two-, three- or four-membered ring).

procedure of de Pablo and co-workers is used to estimate how the Born contribution varies locally throughout the system [14,15]. In this case, the local Born contribution at position $\vec{r}$ is evaluated as

$$C^B_{iiii}(\vec{r}) = \frac{1}{V_{Loc}}\left\{\sum_{\alpha=1}^{N}\sum_{\beta=\alpha+1}^{N}\left(\frac{\partial^2 U}{\partial r_{\alpha\beta}^2} - \frac{1}{r_{\alpha\beta}}\frac{\partial U}{\partial r_{\alpha\beta}}\right)\left(\frac{(x_{\beta,i}-x_{\alpha,i})^4}{r_{\alpha\beta}^2}\right) \times\left(\frac{q_{\alpha\beta}(\vec{r})}{r_{\alpha\beta}}\right)\right\}, \quad (2)$$

where V_{Loc} is the volume of the volume element at position $\vec{r}$, and $q_{\alpha\beta}(\vec{r})/r_{\alpha\beta}$ is the fraction of the vector between atoms α and β that lies within the volume element at $\vec{r}$ ($q_{\alpha\beta}/r_{\alpha\beta}=0$ if the interatomic vector does not pass through the volume element). The contribution from the reciprocal space Ewald sum cannot be divided as in Eq. (2), and so it is split equally among all volume elements (note that the contribution from the reciprocal space Ewald sum to C^B is very small). In this study, the volume elements are slices of the simulation cell that are 1 Å thick. For simulations of the bulk, C^B is obtained as the average of C^B_{1111}, C^B_{2222}, and C^B_{3333}; for the slab

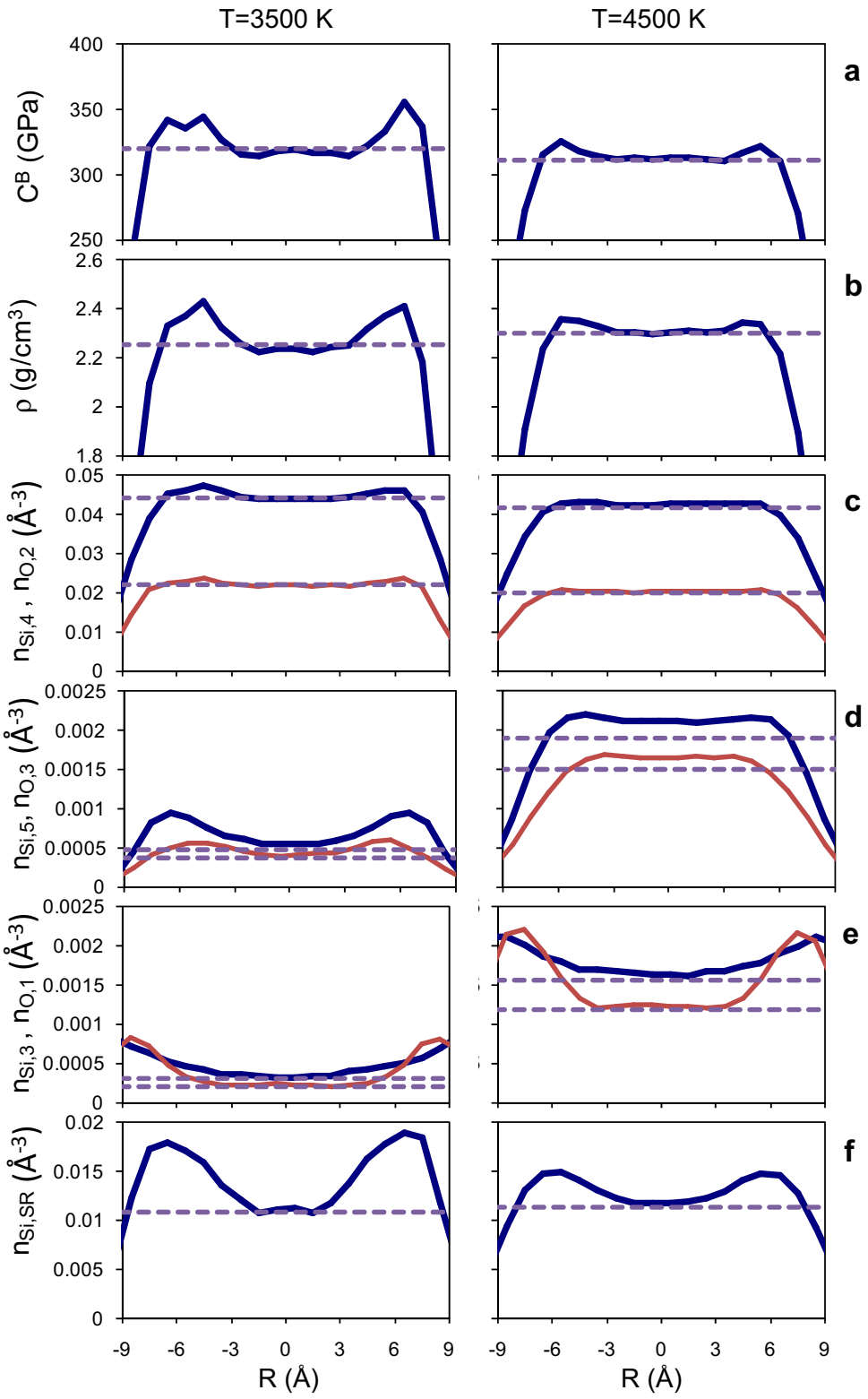

FIG. 2. (Color online) Results for properties as a function of position within the slab, for the slab with thickness of ~17 Å. See Fig. 1 caption for details.

simulations C^B is obtained as the average of C^B_{1111} and C^B_{2222} (the directions perpendicular to the slab surface).

III. RESULTS

For bulk silica, the results for the density at zero pressure are $\rho=2.25$ g/cm^3 at T=3500 K and $\rho=2.30$ g/cm^3 at T=4500 K, which agree with previous results obtained with the same potential [13]. Note that in this temperature range the silica liquid contracts upon heating. The results for the Born contribution to the elasticity of bulk silica are $C^B=320$ GPa at T=3500 K and $C^B=311$ GPa at T=4500 K.

The local ρ and C^B profiles for the silica slabs are shown in Figs. 1–3 [parts (a) and (b)] and compared with the cor-

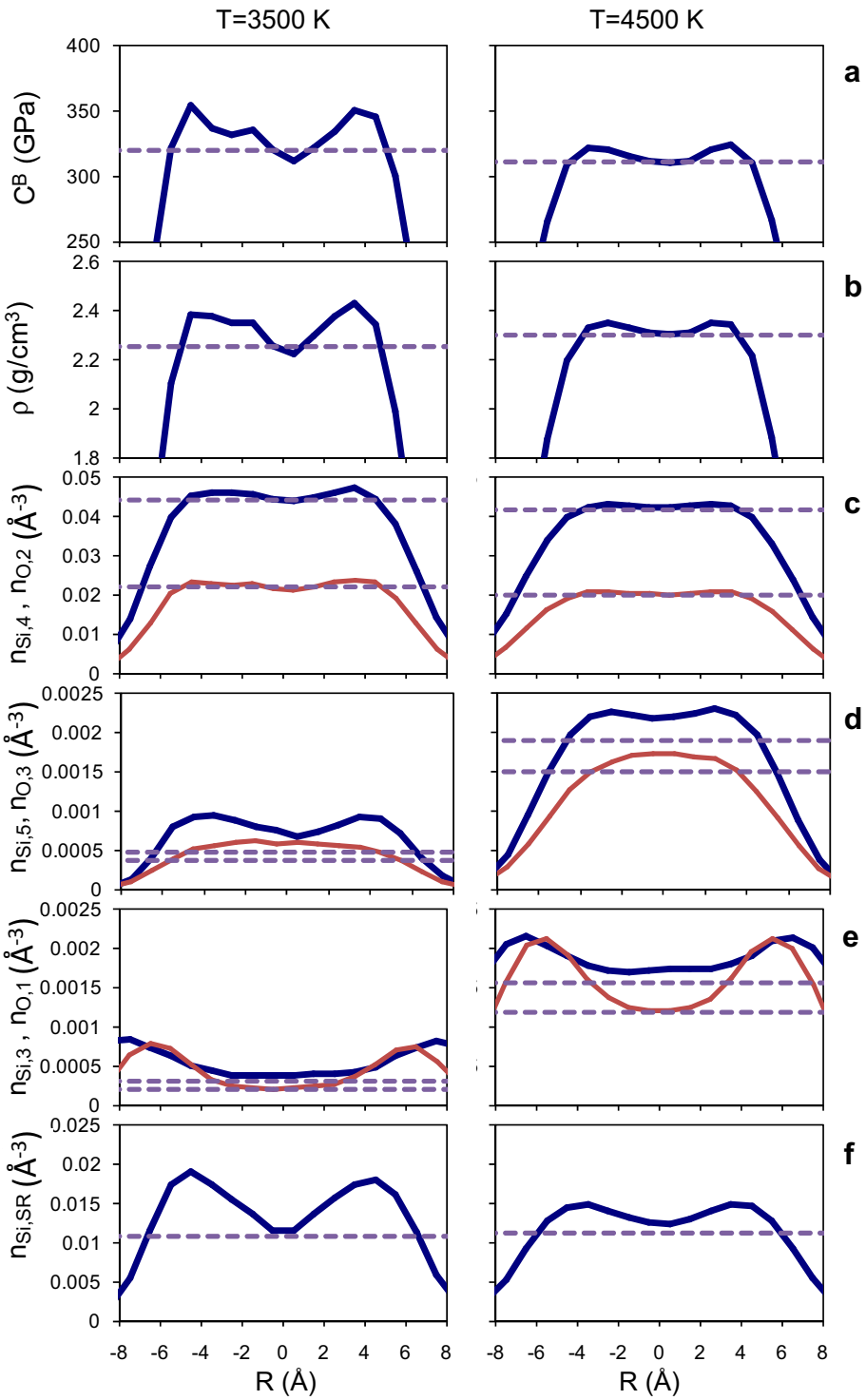

FIG. 3. (Color online) Results for properties as a function of position within the slab, for the slab with thickness of ~13 Å. See Fig. 1 caption for details.

responding bulk properties. For all three slabs, the values of ρ and C^B in the interior of the slab are equal to those of the bulk. However, both ρ and C^B are greater at the edges of the slabs; this effect is much more pronounced at T=3500 K than at T=4500 K.

The ρ and C^B profiles in Figs. 1–3 appear similar, suggesting that these two properties are correlated. As shown in Fig. 4, the local values of ρ and C^B are indeed correlated. Furthermore, the local values of ρ and C^B for bulk silica follow the same correlation. (The variations in the local values of ρ and C^B for the bulk system are due to the sluggishness of the dynamics and the time scale of the simulation; the values would become equal at all locations for long simulation times. Since the dynamics are less sluggish at higher temperature, the variation in the local properties of the bulk system are much smaller at T=4500 K than at T=3500 K).

The kinetic energy contribution to the elastic modulus, C^K, is proportional to the number of atoms in the reference volume [15]. Therefore the profiles of C^K in the slabs will closely mirror the density profiles in Figs. 1–3 (the C^K profiles will differ slightly because C^K is proportional to number density, not mass density), i.e., as with C^B, the values of C^K

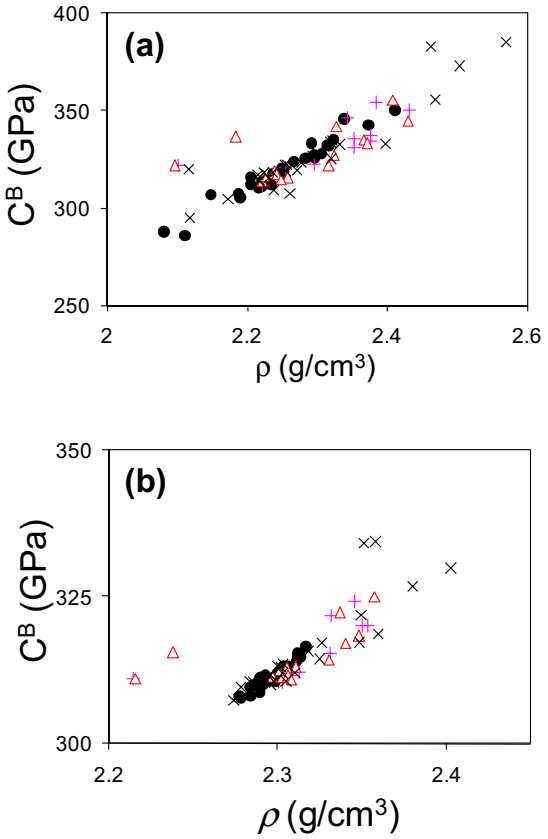

FIG. 4. (Color online) Local Born contribution to the elasticity as a function of local density. (a) $T=3500$ K. (b) $T=4500$ K. Circles: bulk silica; X: slab thickness ~29 Å; triangles: slab thickness ~17 Å; and +: slab thickness ~13 Å.

are greater at the slab edges than in the slab interior. However, the magnitude of C^K is relatively small (for bulk silica at T=3500 K, $C^K=13$ GPa while $C^B=320$ GPa).

The values of ρ and C^B are determined by the atomic level structure, which can be characterized in part by the ion coordination and the ring size distribution. The ion coordination, which characterizes the short-range structure, is dominated by fourfold coordinated Si and twofold coordinated O; in bulk silica, ~98% and ~90% of the ions have this coordination at T=3500 and 4500 K, respectively. The ring size distribution characterizes the intermediate range structure; a ring is defined as the shortest closed loop of Si-O units that leaves a Si ion via one Si-O unit and returns to the same Si ion via a different Si-O unit, and the size of the ring is the number of Si-O units in the ring. For bulk silica, the average ring size is ~6.

The results for the average ion coordination as a function of position in the slabs are shown in Figs. 1–3 [parts (c)–(e)]. In particular, parts (c)–(e) show the number densities of normally coordinated ions (fourfold coordinated Si and twofold coordinated O), highly coordinated ions (fivefold coordinated Si and threefold coordinated O), and less coordinated ions (threefold coordinated Si and onefold coordinated O), respectively. In the slab interior, the ion coordination is very similar to the bulk (but the thinner slabs have a greater concentration of highly coordinated ions even in the slab interior). At the very edge of the slabs, there is a layer with a greater concentration of lower coordinated ions (e.g., dangling oxygen ions). However, just inside this outermost layer, there is a layer with a greater concentration of highly coordinated ions; the position of this layer of highly coordinated ions coincides with the region of increased ρ and C^B described above.

Figures 1–3 [parts (f)] show the number densities of Si ions that are parts of small rings, where a small ring is defined as a two-, three-, or four-membered ring. In the slab interiors, the ring sizes are the same as those for bulk silica. However, the concentration of small rings is higher at the slab edges, which coincides with the region of increased ρ and C^B described above. The higher concentration of small rings agrees with the results of Raman experiments on nanoporous silicas [6] and fumed silica nanoparticles [16], and previous simulations of silica nanoparticles [7].

IV. DISCUSSION AND CONCLUSIONS

The elasticity of liquid silica slabs is shown to be heterogeneous. In particular, the material is stiffer at the slab edges than within the slab interior, due to a distinct atomic level structure characterized by higher density, greater concentration of highly coordinated ions, and smaller silica rings. For wide slabs, the increased stiffness only occurs at the slab edges, and thus does not affect the whole material. However, when the slab thickness approaches 1 nm, the regions of increased stiffness extend throughout the slab.

The relevance of this result is in regard to nanoporous silica materials [1,2], for which the silica framework is only ~1 to 2 nm thick. X-ray scattering experiments show that the walls of the silica framework become thinner as the porosity increases [17]. The present results suggest that as these walls become thinner, zones of high stiffness extend through increasingly large fractions of the silica framework, causing the overall stiffness of the silica framework to increase. This increase in framework stiffness may act to counteract the usual reduction of the elastic modulus with increasing porosity, and thus cause the elastic modulus of the nanoporous material to be relatively insensitive to porosity, as found experimentally [6].

Our previous simulations, using a different methodology, led to a similar conclusion [6]. In the previous analysis, the global (rather than local) elastic modulus was determined for glassy slabs at zero temperature. While this method allowed evaluation of the full elastic modulus (i.e., not just the Born and kinetic energy contributions), the slab volume must be specified in the elastic modulus calculation. However, the slab volume is not uniquely defined (because the determination of the positions of the slab edges are based on arbitrary definitions), which introduces a level of uncertainty to the analysis. In this regard, the present methodology is superior because the local moduli are not dependent on the slab volume.

While the results are obtained for equilibrated liquids at $T\geqslant 3500$ K, the relevance of the results is in regard to glasses at room temperature (as discussed above). As a liquid is cooled, the system dynamics slows, and at the glass transition temperature the system becomes effectively trapped in

the structure of the liquid at that point. Since the magnitude of the increased stiffness at slab edges increases with decreasing temperature (Fig. 1), this effect is expected to be even greater in room temperature glasses.

The structural change near the edge of the slab likely occurs so that the atoms maintain nearly ideal coordination (twofold for oxygen, fourfold for silicon) at the surface. Results for slabs of Lennard-Jones systems do not show a greater density near the slab edges [18,19], which indicates that this type of structural change at the surface is not a generic effect.

Previous work also found that the density is higher at the surfaces of silica clusters and slabs; that this effect has been found with two different force fields [7,9] as well as with *ab initio* molecular dynamics simulations [20] supports its validity. It was also shown that the magnitude of this increased density is greater at lower temperatures [9], as we find here.

ACKNOWLEDGMENTS

This paper was based on work supported by the National Science Foundation (Grant No. DMR-0402867) and the Donors of the Petroleum Research Fund as administered by the American Chemical Society. We thank Jeff Brinker for many important discussions.

[1] C. T. Kresge, M. E. Leonowicz, W. J. Roth, C. J. Vartuli, and J. S. Beck, Nature (London) **359**, 710 (1992).
[2] Y. F. Lu, R. Ganguli, C. A. Drewien, M. T. Anderson, C. J. Brinker, W. Gong, Y. Guo, H. Soyez, B. Dunn, M. H. Huang, and J. I. Zink, Nature (London) **389**, 364 (1997).
[3] J. Wu, X. Liu, and S. H. Tolbert, J. Phys. Chem. B **104**, 11837 (2000).
[4] J. Wu, L. Zhao, E. L. Chronister, and S. H. Tolbert, J. Phys. Chem. B **106**, 5613 (2002).
[5] B. L. Kirsch, X. Chen, E. K. Richman, V. Gupta, and S. H. Tolbert, Adv. Funct. Mater. **15**, 1319 (2005).
[6] H. Fan, C. Hartshorn, T. Buchheit, D. Tallant, R. Assink, R. Simpson, D. J. Lacks, S. Torquato, and C. J. Brinker, Nat. Mater. **6**, 418 (2007).
[7] A. Roder, W. Kob, and K. Binder, J. Chem. Phys. **114**, 7602 (2001).
[8] M. Wilson and T. R. Walsh, J. Chem. Phys. **113**, 9180 (2000).
[9] I. V. Schweigert, K. E. J. Lehtinen, M. J. Carrier, and M. R. Zachariah, Phys. Rev. B **65**, 235410 (2002).
[10] P. G. Debenedetti and F. H. Stillinger, Nature (London) **410**, 259 (2001).
[11] B. W. H. van Beest, G. J. Kramer, and R. A. van Santen, Phys. Rev. Lett. **64**, 1955 (1990).
[12] I. Saika-Voivod, F. Sciortino, and P. H. Poole, Phys. Rev. E **63**, 011202 (2000).
[13] K. Vollmayr, W. Kob, and K. Binder, Phys. Rev. B **54**, 15808 (1996).
[14] K. Yoshimoto, T. S. Jain, K. Van Workum, P. F. Nealey, and J. J. de Pablo, Phys. Rev. Lett. **93**, 175501 (2004).
[15] G. J. Papakonstantopoulos, M. Doxastakis, P. F. Nealey, J.-L. Barrat, and J. J. de Pablo, Phys. Rev. E **75**, 031803 (2007).
[16] T. Uchino, A. Aboshi, S. Kohara, Y. Ohishi, M. Sakashita, and K. Aoki, Phys. Rev. B **69**, 155409 (2004).
[17] B. Smarsly, A. Gibaud, W. Ruland, D. Sturnmayr, and C. J. Brinker, Langmuir **21**, 3858 (2005).
[18] M. Mecke, J. Winkelmann, and J. Fischer, J. Chem. Phys. **107**, 9264 (1997).
[19] D. O. Dunikov, S. P. Malyshenko, and V. V. Zhakhovskii, J. Chem. Phys. **115**, 6623 (2001).
[20] C. Mischler, W. Kob, and K. Binder, Comput. Phys. Commun. **147**, 222 (2002).